

Relaxor ferroelectric behavior and structural aspects of

$\text{SrNaBi}_2\text{Nb}_3\text{O}_{12}$ ceramics

Sunil Kumar,¹ D.A. Ochoa,² J.E. Garcia², and K.B.R. Varma,^{1,a)}

¹ Materials Research Centre, Indian Institute of Science, Bangalore, India 560012.

² Department of Applied Physics, Universitat Politècnica de Catalunya, 08034

Barcelona, Spain.

Abstract

$\text{SrNaBi}_2\text{Nb}_3\text{O}_{12}$ powder was prepared via the conventional solid-state reaction method. X-ray structural studies confirmed the phase to be a three-layered member of the Aurivillius family of oxides. $\text{SrNaBi}_2\text{Nb}_3\text{O}_{12}$ (SNBN) ceramics exhibited the typical characteristics of relaxor ferroelectrics, associated with broad and dispersive dielectric maxima. The variation of temperature of dielectric maxima (T_m) with frequency obeyed the Vogel-Fulcher relationship. Relaxor behavior was believed to be arising from the cationic disorder at A-site. Pinched ferroelectric hysteresis loops were observed well above T_m .

^{a)} Corresponding author; E-Mail: kbrvarma@mrc.iisc.ernet.in, Tel.: +91 80 22932914.

I Introduction

Aurivillius family of oxides have become increasingly important as lead-free ferroelectric materials owing to their superior polarization fatigue resistance characteristics along with high Curie temperatures that make them attractive for nonvolatile memory applications.^{1,2} These bismuth layer-structured ferroelectrics consist of intergrowth of $[\text{Bi}_2\text{O}_2]^{2+}$ layers and $[\text{A}_{n+1}\text{B}_n\text{O}_{3n+1}]^{2-}$ pseudo-perovskite units, where n represents the number of perovskite-like layers stacked along the c -axis. Ferroelectricity in the orthorhombic phase of these compounds is generally attributed to the cationic displacement along the polar a -axis and the tilting of octahedra around the a - and c -axes.³⁻⁵ Though the majority of Aurivillius compounds have normal ferroelectric to paraelectric phase transitions, a few compounds however exhibit relaxor-like diffuse phase transitions.⁶⁻¹¹ Relaxors that are characterized by the frequency dependent diffuse phase transitions, are of significant interest for various applications as these possess exceptionally high dielectric and piezoelectric responses over a wide range of temperatures.^{12,13}

Most literature pertaining to relaxors constitutes the studies on lead-based complex perovskites. In comparison, comprehension of the mechanism underlying the relaxor behavior in Aurivillius compounds is limited. Positional static disorder on A-site as well as the presence of Ba cations in Bi_2O_2 layer associated with the composition fluctuations which result in the formation of nano/micro domains with different structural distortion levels is reckoned to be the possible mechanism for the relaxor behavior in $\text{BaBi}_2(\text{Ta}/\text{Nb})_2\text{O}_9$ and $\text{BaBi}_4\text{Ti}_4\text{O}_{15}$.^{11,13,14} Karthik et al. indeed confirmed the presence of ordered polar regions with 1:1 ordering of A-site cations and accompanied relaxor behavior in $\text{K}_{0.5}\text{La}_{0.5}\text{Bi}_2(\text{Nb}/\text{Ta})_2\text{O}_9$.^{7,8} Investigations concerning

the structural, dielectric and the relaxor characteristics of SrNaBi₂Nb₃O₁₂ (three-layer Aurivillius phase) are reported in the present article. SrNaBi₂Nb₃O₁₂ ceramics exhibited Polarization-electric field (P-E) hysteresis loops at temperature well above the temperature of dielectric maximum (T_m). This behavior is consistent with the existence of polar nano/micro regions above T_m in relaxor ferroelectrics.

II Experimental

Strontium sodium bismuth niobate (henceforth abbreviated as SNBN) powder was synthesized by reacting stoichiometric amounts of reagent grade Na₂CO₃, SrCO₃, Bi₂O₃ and Nb₂O₅ (purity > 99%). The above mixture was ball milled using agate balls in ethanol medium for 4 h, dried and calcined at 1073 K for 5 h and subsequently at 1223 K for 10 h with intermediate grinding. The calcined powder was mixed with a small amount of PVA (polyvinyl alcohol) and the mixture was uniaxially pressed into pellets of about 1-2 mm in thickness and 12 mm in diameter. The binder was burnt out by slowly heating the pellets at 773 K for 5 h. The pressed pellets were sintered at 1323 K for 4 h in air at a heating rate of 3 K/ min and then furnace cooled to room temperature. The monophasic nature of the calcined powders and subsequently sintered pellets was confirmed by X-ray powder diffraction (Bruker-D8 Advance, Cu-K_α radiation) studies. The *FULLPROF* program was used for Rietveld structural refinement. The Bragg peaks were modelled with pseudo-Voigt function and the background was estimated by linear interpolation between selected back-ground points. Scale factor, zero correction, half width parameters, lattice parameters, and positional coordinates were varied during the refinement. Densities of the sintered pellets were measured by the Archimedes method. Xylene (room temperature density ~ 0.86 g/cm³) was used as the liquid medium. Scanning electron microscope (Quanta-

ESEM) was used for microstructural analyses. The high resolution transmission electron microscopic (HRTEM) studies were carried out using a Tecnai-T20 (200 kV) TEM equipped with a double-tilt rotating sample holder. Specimens for TEM were prepared by sonicating the dispersed SNBN powder in acetone medium and putting a droplet of this dispersion on a copper grid coated with carbon thin film. For electrical property measurements, silver electrodes were applied on either side of polished surfaces of pellet and then the sample was baked at 473 K for 2 h to dry out the moisture prior to any measurement. Dielectric response was obtained by using a precision LCR meter (Agilent E4980A) sweeping between 100 Hz and 1 MHz. Samples were placed in a closed loop cold finger cryogenic system in order to scan the temperature between 50 K and 400 K at 1 K min⁻¹. The ferroelectric characteristics; the remnant polarization, maximum polarization and coercive field were determined from the P–E hysteresis loop recorded using a modified Sawyer–Tower circuit (Automated PE loop tracer, Marine India Elect.).

III Results and Discussion

Figure 1(a) shows X-ray powder diffraction pattern, obtained at room temperature, along with the Rietveld refinement profile for SNBN. All the diffraction peaks could be indexed to the space group *B2cb*. The reliability factors R_p , R_{wp} (weighted profile), R_{exp} , χ^2 and the goodness of fit s ($= R_{wp}/R_{exp}$) for the pattern are 5.99%, 8.45%, 4.46%, 3.59% and 1.89, respectively. The refined lattice parameters are: $a = 5.5122(3)$ Å, $b = 5.5093(3)$ Å, and $c = 32.9150(12)$ Å. Pseudo-tetragonality at room temperature in SNBN is expected as the phase transition is in the vicinity of room temperature and microscopic polar regions are indeed present even above the phase transition temperature (discussed latter in the text). It should be mentioned here that the choice

of orthorhombic $B2cb$ space group was in light of the observations that odd-layered Aurivillius compounds tend to crystallize in $B2cb$ space group in their ferroelectric state and the incidence of a ferroelectric hysteresis loop at room temperature confirm the ferroelectric nature of SNBN. Detailed structural analysis for the SNBN goes beyond the scope of the present investigation and remains to be addressed to in future work. The lattice image recorded along the $[100]$ zone axis is shown in the Fig. 1(b). Regular stacking of the slabs at a periodicity of ~ 1.65 nm which corresponds to the half of the c lattice parameter of the orthorhombic unit cell establishes the layered structure of the present compound. The scanning electron micrograph recorded for the pellet sintered at 1323 K for 4 h in air is shown in Fig. 1(c). The micrograph shows the presence of well-packed and randomly oriented **platelet-like** grains with an average size of ~ 10 μm . Energy dispersive X-ray analyses (EDX) carried out on various grains of the sample confirmed the composition to be $\text{SrNaBi}_2\text{Nb}_3\text{O}_{12}$ within the typical error associated with EDX analysis. The relative density of this pellet was around 95% of theoretical density. This disc-like morphology is indeed a characteristic feature of the Aurivillius family of compounds and is attributed to their strong anisotropic nature.¹⁶

Temperature dependence of the real (ϵ_r') and imaginary (ϵ_r'') parts of the dielectric constant for the SNBN sample at selected frequencies in the range 100 Hz - 1MHz is depicted in Fig. 2. Dielectric data was collected during heating the sample with a constant heating rate of 1 K/min. Diffuse phase transition associated with strong frequency dispersion is observed in both ϵ_r' and ϵ_r'' curves, suggesting the relaxor nature of SNBN ceramics. The magnitude of ϵ_r' decreases with increasing frequency and the temperature of dielectric maximum T_m , corresponding to the maximum value of ϵ_r' , shifts towards higher temperature. A shift of 25 K in T_m with increase in

frequency from 100 Hz to 1 MHz is observed. Similar shift in T_m and an increase in maximum value of ϵ_r'' are also observed with increasing frequencies. To quantify the diffuseness of phase transition, a modified Curie–Weiss law given by $1/\epsilon_r' - 1/\epsilon_m = C^{-1}(T - T_m)^\gamma$ is used;¹⁷ where ϵ_m is the dielectric constant at T_m , C is the Curie-like constant and γ ($1 \leq \gamma \leq 2$) is the degree of diffuseness. By fitting the experimental data in modified Curie-Weiss law, γ is found to be 1.67 ± 0.01 (at 100 kHz) corroborating the diffused phase transition behavior of SNBN ceramics.

Relaxor ferroelectrics are known to follow an empirical Vogel–Fulcher (VF) relationship,¹⁸ $f = f_0 \exp[-E_a/k(T_m - T_{VF})]$, where E_a and T_{VF} are the activation energy and the static freezing temperature, k is the Boltzmann constant and f_0 is the pre-exponential factor. Figure 3 shows the variation of T_m with $\ln(f)$ for the SNBN ceramics. From the non-linear VF fitting of ϵ_r' [Fig. 3], values of the fitting parameters f_0 , E_a and T_{VF} were found to be 1.1×10^8 Hz, 16.2 ± 0.7 meV and 281.1 ± 0.6 K, respectively. The values of activation energy and static freezing temperature for SNBN are comparable to that of conventional lead-based relaxor $\text{Pb}(\text{Mg}_{1/3}\text{Nb}_{2/3})\text{O}_3$ ($T_{VF} \sim 291$ K and $E_a \sim 40$ meV).¹⁸ Comparison with the other relaxors belonging to Aurivillius family of oxides shows that T_{VF} for the present compound is significantly lower than that for $\text{BaBi}_4\text{Ti}_4\text{O}_{15}$ ¹⁹ and $\text{K}_{0.5}\text{La}_{0.5}\text{Bi}_2(\text{Nb}/\text{Ta})_2\text{O}_9$.^{7,8} and higher than the static freezing temperature reported for $\text{BaBi}_2\text{Nb}_2\text{O}_9$.⁶ The activation energy of frequency dispersion for $\text{BaBi}_2\text{Nb}_2\text{O}_9$ is about 0.6 eV and $T_m - T_{VF}$ is about 300 K (at 1 kHz). In comparison, for SNBN the value of $T_m - T_{VF}$ difference (19 K, at 1 kHz) is much smaller and it is comparable to that of $\text{Pb}(\text{Mg}_{1/3}\text{Nb}_{2/3})\text{O}_3$ (23 K).¹⁸

Relaxor-like behavior occurs mainly because of the local compositional fluctuations and/or structural disorder in the arrangement of cations in one or more crystallographic sites of the structure.^{12,20} However, many Aurivillius phases have atomic positions with a mixed occupancy on the A and/or B site of the perovskite blocks but without being associated with a relaxor behavior.^{14,15} For SNBN, Na⁺ and Sr²⁺ occupy the A-site of the perovskite blocks in 50:50 ratio. Disorder at the A-site of perovskite blocks due to the random distribution of Sr²⁺ and Na⁺ seems to be responsible for observed relaxor behavior in SNBN. A-site disorder and associated relaxor properties have been observed in perovskite Na_{0.5}Bi_{0.5}TiO₃, as well as in two-layered Aurivillius phases K_{0.5}La_{0.5}Bi₂(Nb/Ta)₂O₉.^{7,8,21}

Room temperature (295 K) P-E loop recorded at a frequency of 50 Hz for SNBN ceramics is shown in Fig. 4(a). A remnant polarization ($2P_r$) of 4.1 $\mu\text{C}/\text{cm}^2$, maximum polarization ($2P_{max}$) of 15.1 $\mu\text{C}/\text{cm}^2$ and a coercive field ($2E_C$) of 28.3 kV/cm were obtained under a maximum applied electric field of 88 kV/cm. Unlike normal ferroelectrics for which polarization becomes zero at the Curie temperature T_C , relaxor ferroelectrics are known to possess non-zero polarization at temperatures well above T_m which is attributed to the presence of micro/nanoscale polar regions.¹² It is widely believed that these polar nano/micro regions are responsible for the relaxor behavior. Several models have been proposed for the mechanism of formation of microscopic polar regions.^{12,18,21-31} Formation of these polar regions occurs at T_B , so called Burns temperature (analogue of the freezing of the spin fluctuations in a magnetic system), which could be hundreds of degrees higher than T_m .³¹ At temperature close to T_B , these polar regions are in ergodic state. Upon cooling, dynamics of polar regions slow down and finally freeze at $T_{VF} < T_m$.²² To corroborate the presence of spontaneous polarization above the phase transition, P-E loops

recorded at three different temperatures (above T_m) are shown in Figs. 4 (b)-(d). At these temperatures P-E loop becomes pinched (or constricted). Pinched P-E loops have also been observed in compounds with antiferroelectric component and also in doped-ferroelectrics after ageing.³²⁻³⁴ This phenomenon in acceptor-doped ferroelectrics is considered to relate to defect dipoles providing a restoring force to polarization reversal, thus ‘pinning’ the motion of ferroelectric domains.³³ However, ageing related phenomena do not seem to be responsible for the constricted loops observed in our sample. While it is true that some amount of oxygen vacancies are generally present in Aurivillius family of oxides due to volatilization of bismuth during high temperature sintering but for the present sample pinching of hysteresis loop is more pronounced above T_m whereas no pinching is apparent in the hysteresis loop recorded at 295 K (Fig. 4). Reversibility in temperature dependent shape of P-E loops indicates that such a behavior in SNBN might arise due to the coexistence of polar and non-polar regions at these temperatures.

IV Conclusions

We have investigated the structural and relaxor behavior of $\text{SrNaBi}_2\text{Nb}_3\text{O}_{12}$ ceramics. The Rietveld refinement of X-ray powder data suggests that SNBN crystallizes in the orthorhombic space group $B2cb$. SNBN ceramics exhibited near-room temperature frequency-dependent dielectric maximum which follows the Vogel-Fulcher relation implying a relaxor nature. The relaxor behavior seems to have its origin in inhomogeneous distribution of Na^+ and Sr^{2+} at A-site. Pinched P-E loops were observed well above T_m .

Acknowledgements

One of the authors (S.K.) is grateful to the Council of Scientific and Industrial Research (CSIR), New Delhi, for the award of Senior Research Fellowship. S.K. also thanks the European Commission for providing fellowship through EMECW-WILLpower programme to carry out some of the present investigations at UPC, Barcelona, Spain.

References:

1. B. H. Park, B. S. Kang, S. D. Bu, T. W. Noh, J. Lee, and W. Jo, "Lanthanum-substituted bismuth titanate for use in non-volatile memories" *Nature*, **401**, 682 (1999).
2. M. D. Maeder, D. Damjanovic, and N. Setter, "Lead-free piezoelectric materials," *J. Electroceram.*, **13**, 385–92 (2004).
- 3 B. Aurivillius, "Mixed Bismuth Oxides with Layer Lattices: I. The Structure Type of $\text{CaNb}_2\text{Bi}_2\text{O}_9$," *Ark. Kemi.* **1**, 463-80 (1949); "Mixed Bismuth Oxides with Layer Lattices: II. Structure of $\text{Bi}_4\text{Ti}_3\text{O}_{12}$," 499-512 (1949).
4. E. C. Subbarao, "Crystal chemistry of mixed bismuth oxides with layer-type structure," *J. Am. Ceram. Soc.* **45**, 166-169 (1962).
5. R. E. Newnham, R. W. Wolfe, and J. F. Dorrian, "Structural basis of ferroelectricity in the bismuth titanate family," *Mat. Res. Bull.*, **6**, 1029-1040 (1971).
- 6 A. L. Kholkin, M. Avdeev, M. E. V. Costa, J. L. Bapista, and S. N. Dorogovtsev, "Dielectric Relaxation in Ba-Based Layered perovskites," *Appl. Phys. Lett.*, **79**, 662–4 (2001).
7. C. Karthik, N. Ravishankar, Mario Maglione, R. Vondermuhil, J. Etoueau, and K.B.R. Varma, " Relaxor behavior of $\text{K}_{0.5}\text{La}_{0.5}\text{Bi}_2\text{Nb}_2\text{O}_9$ ceramics," *Appl. Phys. Lett.* **89**, 042905 (2006).
8. C. Karthik, N. Ravishankar, Mario Maglione, R. Vondermuhil, J. Etoueau, and K.B.R. Varma, "Relaxor behavior of $\text{K}_{0.5}\text{La}_{0.5}\text{Bi}_2\text{Ta}_2\text{O}_9$ ceramics," *Solid State Commun.* **139**, 268 (2006).
9. R. Z. Hou, X. M. Chen, and Y. W. Zeng, "Diffuse Ferroelectric Phase Transition and Relaxor Behaviors in Ba-Based Bismuth Layer-Structured Compounds and La-Substituted $\text{SrBi}_4\text{Ti}_4\text{O}_{15}$," *J. Am. Ceram. Soc.*, **89** [9], 2839-2844 (2006).

10. X. B. Chen, R. Hui, J. Zhu, W. P. Lu, and X. Y. Mao, "Relaxor properties of lanthanum-doped bismuth layer-structured ferroelectrics," *J. Appl. Phys.*, **96**, 5697-700 (2004).
11. Ismunandar and B. K. Kennedy, "Structure of $ABi_2Nb_2O_9$ ($A= Sr, Ba$): Refinement of Powder Neutron Diffraction Data," *J. Solid State Chem.*, **126**, 135-41 (1996).
12. L. E. Cross, "Relaxor Ferroelectrics," *Ferroelectrics*, **76**, 241-67 (1987).
13. Z.-G. Ye, "Relaxor Ferroelectric Complex Perovskites: Structure, Properties and Phase Transitions," *Key Eng. Mater.*, **155**, 81-122 (1998).
14. J. Tellier, Ph. Boullay, D. B. Jennet, and D. Mercurio, "Structural evolution in three and four-layer Aurivillius solid solutions: A comparative study versus relaxor properties," *Solid State Sci.*, **10** [2], 177-185 (2008).
15. J. Tellier, Ph. Boullay, M. Manier, and D. Mercurio, "A comparative study of the Aurivillius phase ferroelectrics $CaBi_4Ti_4O_{15}$ and $BaBi_4Ti_4O_{15}$," *J. Solid State Chem.*, **177** [6], 1829-37 (2004).
16. J. A. Horn, S. C. Zhang, U. Selvaraj, G. L. Messing, and S. Trolier-McKinstry, "Templated Grain Growth of Textured Bismuth Titanate," *J. Am. Ceram. Soc.*, **82** [4] 921-6 (1999).
17. K. Uchino and S. Namura, "Critical Exponents of the Dielectric Constants in Diffuse-Phase Transition Crystals," *Ferroelectric Lett.*, **44**, 55-61 (1982).
18. D. Viehland, S.G. Jang, L.E. Cross and M. Wuttig, "Freezing of the polarization fluctuations in lead magnesium niobate relaxors," *J. Appl. Phys.*, **68**, 2916-21 (1990).
19. S. Kumar and K.B. R. Varma, "Influence of lanthanum doping on the dielectric, ferroelectric and relaxor behaviour of barium bismuth titanate ceramics," *J. Phys D: Appl. Phys.*, **42** [7], 075405 9pp. (2009).

20. G. A. Smolenskii, V. A. Isupov, A. I. Agranovskaya, and S. N. Popov, "Ferroelectrics with Diffuse Phase Transitions," *Sov. Phys. Solid State*, **2**[11] 2584 (1961).
21. G. O. Jones and P. A. Thomas, "Investigation of the structure and phase transitions in the novel A-site substituted distorted perovskite compound $\text{Na}_{0.5}\text{Bi}_{0.5}\text{TiO}_3$," *Acta Crystallogr., Sect. B: Struct. Sci.*, **58**, 168-78 (2002).
22. A. A. Bokov and Z.-G. Ye, "Recent progress in relaxor ferroelectrics with perovskite structure," *J. Mater. Sci.*, **41**, 31-52 (2006).
23. R. Blinc, V. Laguta, and B. Zalar, "Field cooled and zero field cooled 207Pb NMR and the local structure of relaxor $\text{PbMg}_{1/3}\text{Nb}_{2/3}\text{O}_3$," *Phys. Rev. Lett.*, **91**[24] 247601/1-01/4 (2003).
24. W. Dmowski, S. B. Vakhrushev, I. K. Jeong, M. P. Hehlen, F. Trouw, and T. Egami, "Local lattice dynamics and the origin of the relaxor ferroelectric behavior," *Phys. Rev. Lett.*, **100**[13] (2008).
25. P. M. Gehring, S. Wakimoto, Z. G. Ye, and G. Shirane, "Soft mode dynamics above and below the Burns temperature in the relaxor $\text{Pb}(\text{Mg}_{1/3}\text{Nb}_{2/3})\text{O}_3$," *Phys. Rev. Lett.*, **87**[27 I] 2776011-14 (2001).
26. A. E. Glazounov and A. K. Tagantsev, "Direct evidence for Vögel-Fulcher freezing in relaxor ferroelectrics," *Appl. Phys. Lett.*, **73**[6] 856-58 (1998).
27. R. Pirc and R. Blinc, "Spherical random-bond-random-field model of relaxor ferroelectrics," *Phys. Rev. B*, **60**[19] 13470-78 (1999).
28. D. Viehland, S. J. Jang, L. E. Cross, and M. Wuttig, "Deviation from Curie-Weiss behavior in relaxor ferroelectrics," *Phys. Rev. B*, **46**[13] 8003-06 (1992).

29. V. Westphal, W. Kleemann, and M. D. Glinchuk, "Diffuse phase transitions and random-field-induced domain states of the relaxor ferroelectric $\text{PbMg}_{1/3}\text{Nb}_{2/3}\text{O}_3$," *Phys. Rev. Lett.*, **68**[6] 847-50 (1992).
30. G. Xu, J. Wen, C. Stock, and P. M. Gehring, "Phase instability induced by polar nanoregions in a relaxor ferroelectric system," *Nature Materials*, **7**[7] 562-66 (2008).
31. G. Burns and F. H. Dacol, "Crystalline ferroelectrics with glassy polarization behavior," *Phys. Rev. B*, **28**, 2527-30 (1983).
32. G. H. Haertling, "Ferroelectric Ceramics: History and Technology," *J. Am. Soc. Ceram.*, **82**, 797-818 (1999).
33. X. Ren, "Large electric-field-induced strain in ferroelectric crystals by point-defect-mediated reversible domain switching," *Nature Mater.*, **3**, 91-4 (2004).
34. A. Singh and R. Chatterjee, "Structural, electrical, and strain properties of stoichiometric $1-x-y(\text{Bi}_{0.5}\text{Na}_{0.5})\text{TiO}_3-x(\text{Bi}_{0.5}\text{K}_{0.5})\text{TiO}_3-y(\text{Na}_{0.5}\text{K}_{0.5})\text{NbO}_3$ solid solutions," *J. Appl. Phys.*, **109**, 024105 5pp. (2011).

Figure captions:

Figure 1. (a) Observed (circles), calculated (solid line), and difference profile (bottom line) obtained from the Rietveld refinement of X-ray powder diffraction profile for $\text{SrNaBi}_2\text{Nb}_3\text{O}_{12}$ using $B2cb$ space group. The vertical bars are the Bragg positions of the reflections in the space group $B2cb$. (b) High resolution transmission electron micrograph recorded along the $[100]$ zone axis. (c) Scanning electron micrograph of fractured surface of the ceramic sintered at 1323 K for 4 h.

Figure 2. Temperature dependence of real (ϵ_r') and imaginary (ϵ_r'') parts of dielectric constant at different frequencies.

Figure 3. Temperature of dielectric maximum T_m as a function of $\ln(f)$ (*spheres* represent the experimental data and the *solid line* is the fit to the Vogel–Fulcher relation).

Figure 4. (a) Polarization vs Electric field hysteresis loop recorded at 295 K, (b) 330 K, (c) 350 K, and (d) 370 K for SNBN ceramics.

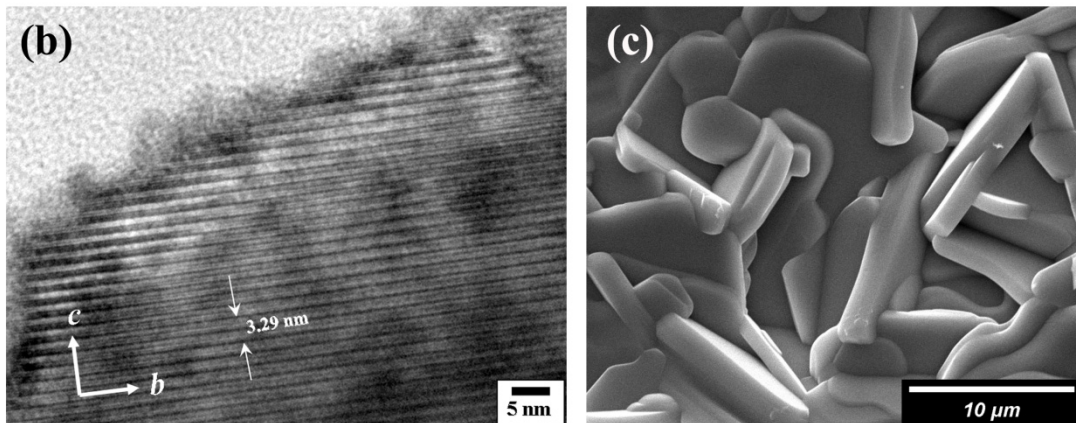
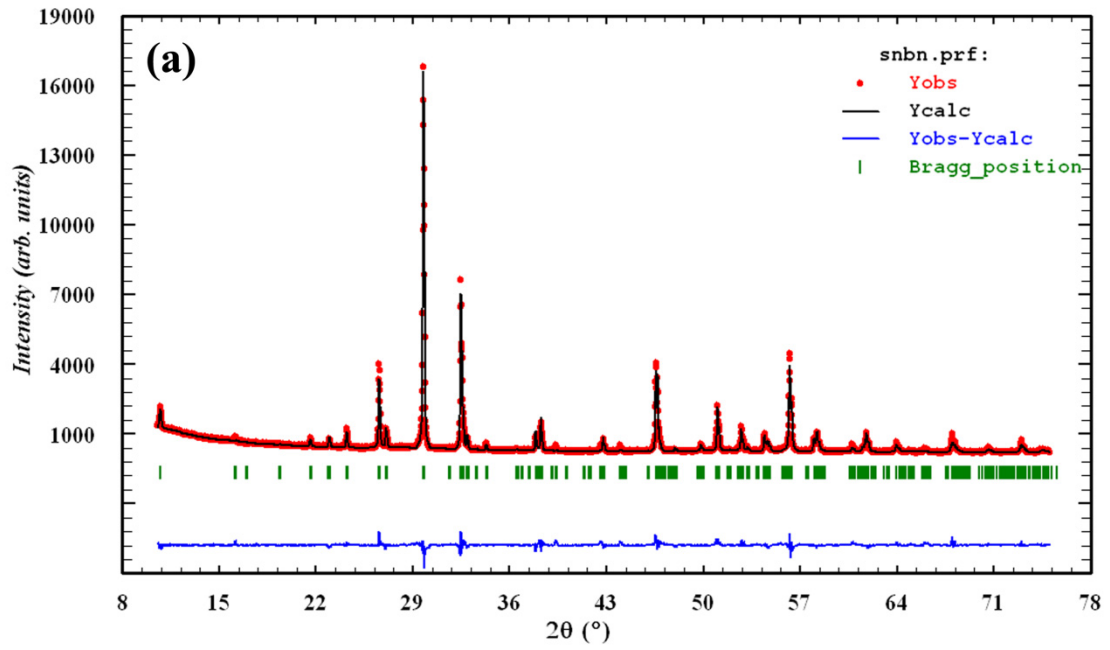


Figure 1

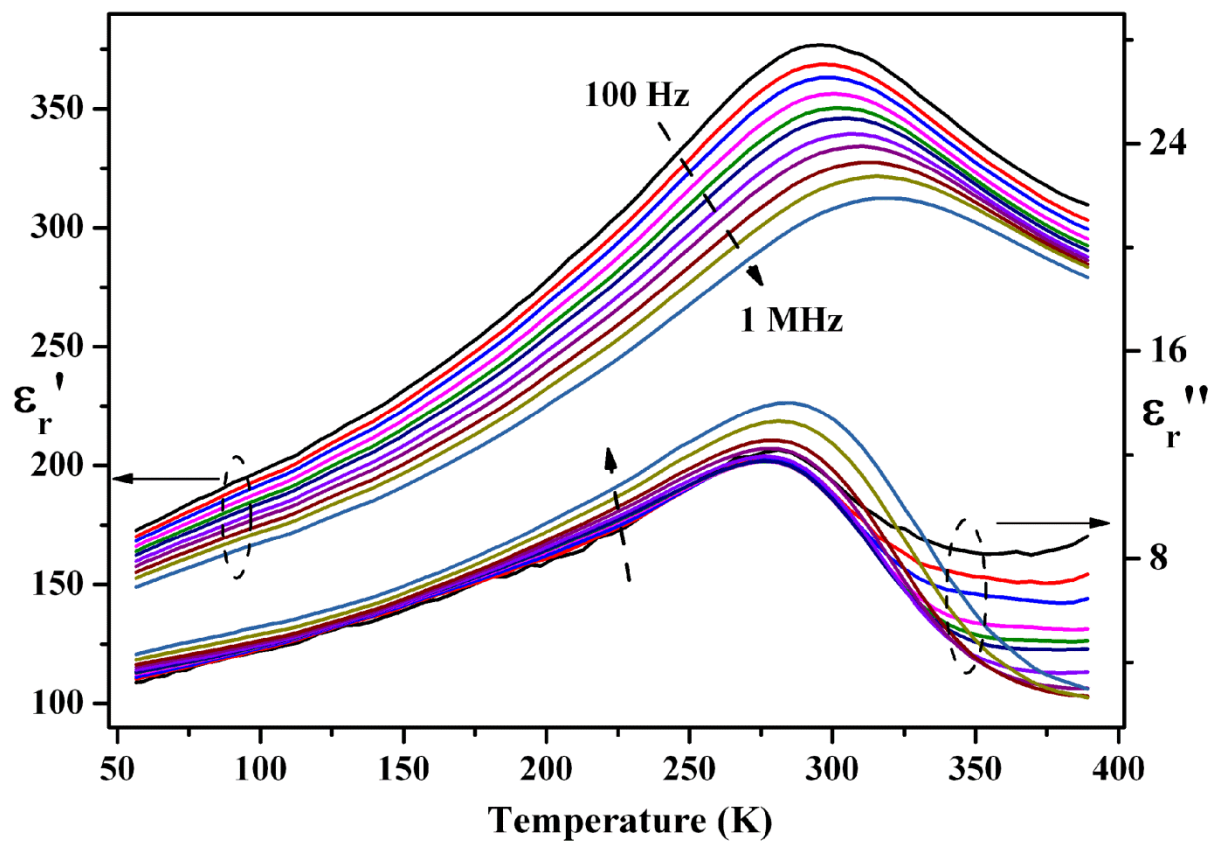


Figure 2

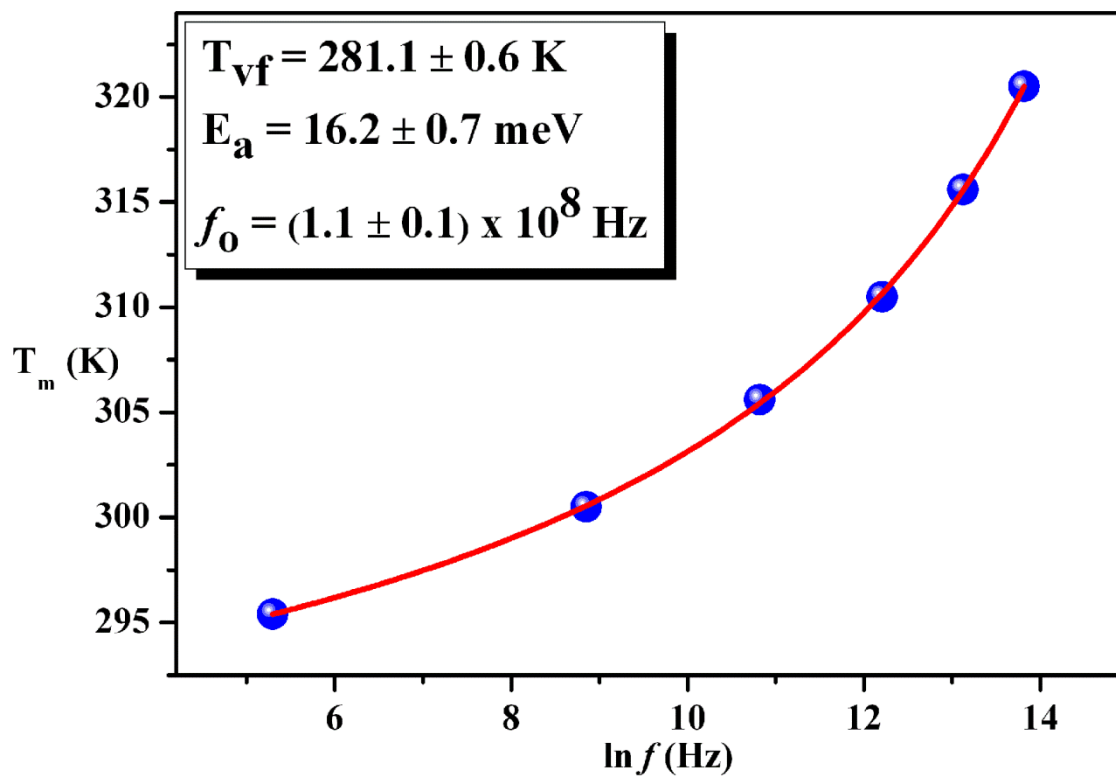


Figure 3

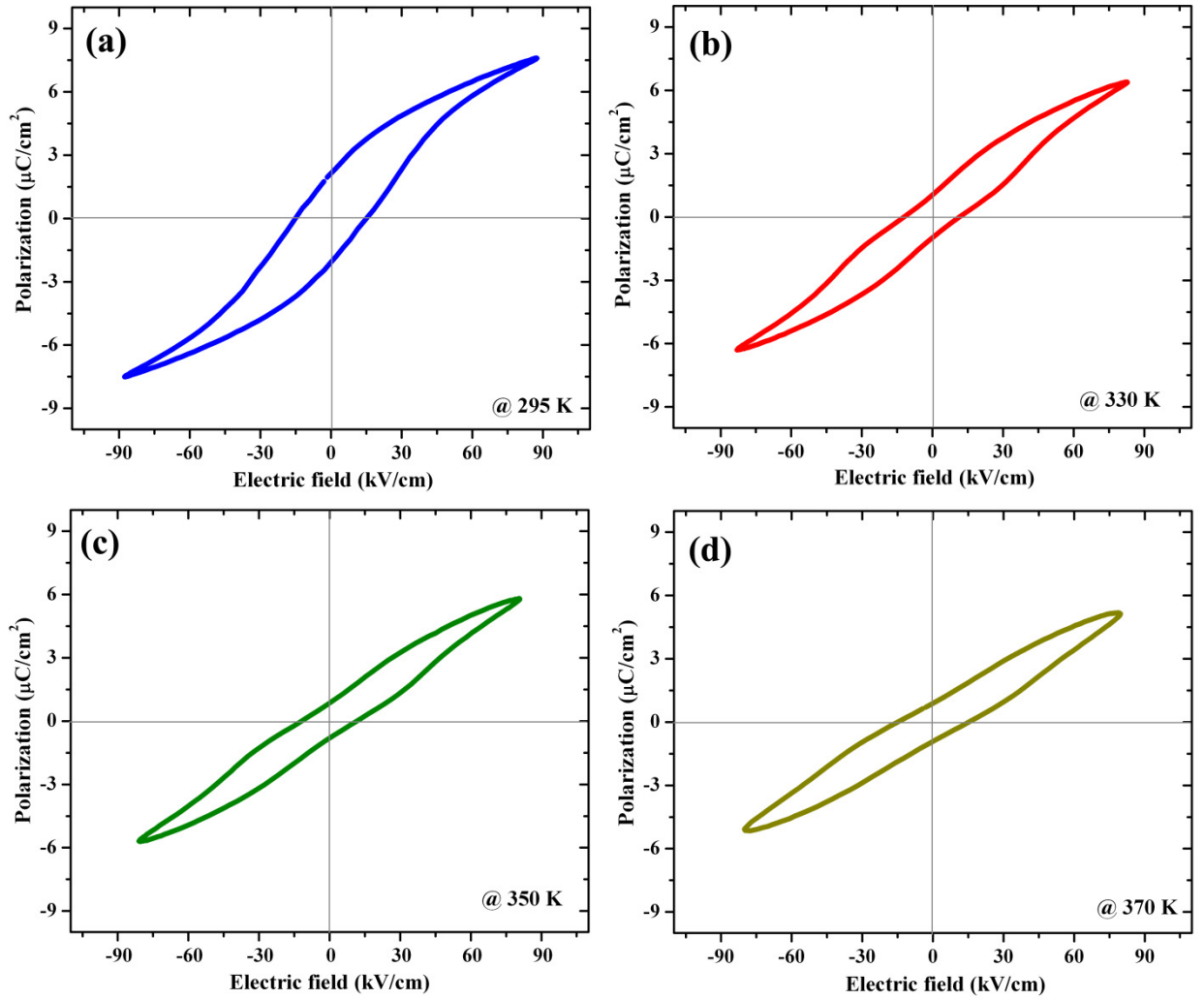


Figure 4